Article

Tissue-Mimicking Gel Phantoms for Thermal Therapy Studies

Ultrasonic Imaging
1–26

DOI: 10.1177/0161734614526372
ultrasonicimaging.sagepub.com

Ali Dabbagh[1,2], Basri Johan Jeet Abdullah[1,2], Chanthiriga Ramasindarum[3,4], and Noor Hayaty Abu Kasim[3,5]

Abstract

Tissue-mimicking phantoms that are currently available for routine biomedical applications may not be suitable for high-temperature experiments or calibration of thermal modalities. Therefore, design and fabrication of customized thermal phantoms with tailored properties are necessary for thermal therapy studies. A multitude of thermal phantoms have been developed in liquid, solid, and gel forms to simulate biological tissues in thermal therapy experiments. This article is an attempt to outline the various materials and techniques used to prepare thermal phantoms in the gel state. The relevant thermal, electrical, acoustic, and optical properties of these phantoms are presented in detail and the benefits and shortcomings of each type are discussed. This review could assist the researchers in the selection of appropriate phantom recipes for their in vitro study of thermal modalities and highlight the limitations of current phantom recipes that remain to be addressed in further studies.

Keywords

thermal gels, hyperthermia, thermal ablation, tissue equivalency, thermal stability

Introduction

Thermal therapy methods, similar to any other therapeutic or diagnostic technique, need assessment and verification in terms of their effectiveness and limitations prior to application in clinical setting. The ideal medium for experimental studies of temperature-based therapies is the real tissue of clinical interest due to the provision of the closest approximation to the clinical conditions. However, in vivo measurements as well as in vitro utilization of real tissues may cause substantial difficulties in preparation, handling, storage, and, particularly, standardization of the results. Therefore, availability of artificial phantoms that closely mimic the physical and

[1]Department of Biomedical Imaging, Faculty of Medicine, University of Malaya, Kuala Lumpur, Malaysia
[2]University of Malaya Research Imaging Centre, University of Malaya, Kuala Lumpur, Malaysia
[3]Biomaterials Technology Research Group, Faculty of Dentistry, University of Malaya, Kuala Lumpur, Malaysia
[4]Dental Research Management Centre, Faculty of Dentistry, University of Malaya, Kuala Lumpur, Malaysia
[5]Department of Restorative Dentistry, Faculty of Dentistry, University of Malaya, Kuala Lumpur, Malaysia

Corresponding Author:
Ali Dabbagh, Department of Biomedical Imaging, Faculty of Medicine, University of Malaya, Kuala Lumpur, 50603, Malaysia.
Email: dabbagh_ali2003@yahoo.com

geometrical properties of target tissues plays an important role in pre-clinical evaluation of thermal modalities.

Although a number of phantoms are available commercially (e.g., from Computerized Imaging Reference Systems Inc., Gammex Inc., and ATS laboratories Inc.), these products are generally constructed for broad applications such as calibration of imaging devices as well as training purposes and may not be suitable for specific requirements. These phantoms may possess insufficient thermal stability or unfavorable physical properties at increased temperatures, which would render them inappropriate for high-temperature experiments. Moreover, uniformity may not exist among laboratories in terms of fundamental properties of a specific tissue-mimicking media[1-3]; that is, a tissue-mimicking phantom designed in a specific laboratory setup may not exhibit similar characteristics when reproduced in a different experimental condition. Hence, many attempts have been made for the development and customization of thermal phantoms to simulate biological tissues at desired experimental conditions (frequency, temperature, etc.). As a result, various recipes have been suggested in liquid, solid, and gel (semisolid) forms. However, gel phantoms have found more popularity because of representing a wide range of thermal, electrical, acoustic, and optical properties. Facile formability is another particular feature of gel phantoms that provides the ability to reproduce realistic irradiation geometries.

This article presents a comprehensive review of the materials used in fabrication of gel phantoms for hyperthermia and thermal ablation investigations. In the subsequent sections, the critical tissue (or phantom) parameters that significantly influence the outcome of different thermal therapeutic techniques are first explained, followed by describing common gelling agents used to develop thermal phantom gels. This review intends to provide a better understanding of the advantages and limitations of various gel phantoms developed for hyperthermia and thermal ablation applications to aid researchers in appropriate selection of a material for their own study.

Critical Phantom Parameters for Thermal Therapy Studies

The physical and geometrical properties of phantoms are customized according to their intended application. Therefore, a phantom fabricated for a particular thermal therapeutic technique is likely to differ from those developed for application in other types of thermal modalities. The required properties of phantom materials even differ in various experimental setups applied for evaluation of a specific thermal modality. Table 1 lists the most significant physical characteristics of the biological tissues that need to be reproduced by thermal phantoms in the four major thermal modalities including High Intensity Focused Ultrasound (HIFU), Radiofrequency (RF), Microwave (MW), and Laser-induced thermal ablation (LIT). Although the thermal profile of the target medium (e.g., tissue or phantom) during treatment with different thermal modalities is mostly governed by the parameters presented in this table, a number of other physical parameters may also influence the treatment outcome. For instance, the nonlinearity parameter (B/A: a measure of density changes in a material in response to the pressure alteration),[39] the backscattering coefficient (the differential scattering cross-section per unit volume for a scattering angle of 180°), and longevity (a time period over which the acoustic and mechanical properties are stable) are additional factors affecting the HIFU outcome.[40] On the contrary, the tissue electrical impedance[41] and relaxation time constants[29] (which explain the time that tissue needs to return to equilibrium conditions) may influence the efficiency of RF and MW therapies, respectively. In LIT experiments, the optical penetration depth (δ: a material thickness at which the light attenuates to 1/e of its initial value) is an influential parameter, determining the characteristic depth to which the target medium is heated. When scattering is negligible, the δ value is given by the reciprocal of the absorption coefficient; whereas, at wavelengths where optical scattering is significant, the

Table 1. Critical Parameters of Thermal Phantoms in Different Thermal Modalities.

Parameter	Symbol	Unit	Definition	References
Common thermal parameters				
Density	ρ	$kg \cdot m^{-3}$	—	
Specific heat capacity	C	$J \cdot kg^{-1} \cdot K^{-1}$	—	4,6
Thermal conductivity	k (or λ, κ)	$W \cdot m^{-1} \cdot K^{-1}$	—	4,6-9
Thermal diffusivity	D (or a, k)	$m^2 \cdot s^{-1}$	—	4,10
HIFU				
Speed of sound in the medium	c	$m \cdot s^{-1}$	—	6,11-13
Characteristic acoustic impedance	Z_0	Rayls	Ratio of effective sound pressure and the particle velocity at a point in a free, progressive wave.	14,15
Attenuation coefficient	α	$dB \cdot cm^{-1} \cdot MHz^{-1}$	The extent of reduction in acoustic intensity when passing through the medium.	6,11,13,16
The (inertial) cavitation threshold	P_{cav}	Pa	The minimum rarefactional pressure required to induce cavitation at a specified frequency.	17,18
RF and MW				
Specific absorption rate	SAR	$W \cdot kg^{-1}$	Time rate of electromagnetic energy deposition per unit mass.	19-23
Electrical conductivity	σ (or κ)	$S \cdot m^{-1}$	—	10,24
Complex permittivity	ε	$F \cdot m^{-1}$	The resistance against formation of an electric field in the medium	25-29
Real part of permittivity	ε'	$F \cdot m^{-1}$	Medium's ability to store electric field energy.	25,29
Imaginary part of permittivity (loss factor)	ε''	$F \cdot m^{-1}$	A measure of the dissipated energy in the material.	25,26,29
Loss tangent (tan δ)	$\varepsilon'/\varepsilon''$	—	A measure of loss-rate of electrical energy in the system.	10,25,29
Relative permittivity	ε_r (or $\frac{\varepsilon}{\varepsilon_0}$)	—	Medium's normalized permittivity according to vacuum	5,10,25,27,29
Dielectric constant (real part of relative permittivity)	ε_r' (or $\frac{\varepsilon'}{\varepsilon_0}$)	—	Ratio of the stored electrical energy in the material by a given voltage, relative to that in vacuum.	25,29,30
Laser				
Diffusion coefficient	D	$cm^2 \cdot s^{-1}$	Proportionality constant between the light transfer rate and the light intensity gradient	31-36
Light absorption coefficient	μ_a	m^{-1}	Probability of photon absorption in unit length of medium.	31-38
Reduced scattering coefficient	μ_s'	m^{-1}	Describes the diffusion of photons in a random path of step size of $1/\mu_s'$	31-38
Light scattering coefficient	μ_s	m^{-1}	Probability of photon scattering in unit length of medium.	31-38
Anisotropy factor	g	—	Represents the effects of directionally dependent scattering	31-36

HIFU = High Intensity Focused Ultrasound; RF = radiofrequency; MW = microwave.

δ value is smaller than $1/\mu_a$.[33] However, because of difficulties in accurate measurement of the above-mentioned parameters in most laboratories, these values are rarely reported in the relevant literature.

It is also noteworthy that the thermal, acoustic, electrical, and optical properties of biological tissues drastically depend on the external conditions such as temperature and applied frequency. The magnitude of this dependence also varies among different tissues. Therefore, a desirable phantom material must mimic the target tissue properties over wide temperature and frequency ranges. It is also ideal that the phantoms simultaneously mimic all thermal, acoustic, electrical, and optical properties of human tissues. However, development of such phantoms remains a challenging area of research in the field of thermal therapy.

Table 2. The Ingredients (% w/w) and Various Properties of TX-150-Based Thermal Phantoms Suggested in Literature.

	Guy (1971)[19]	Cheung and Koopman (1976)[43]	
TX-150 (or TX-151)	8.40	8.45	
Polyethylene powder	15.20	15.20	
NaCl	~0.92[a]	0.91	
Water	the rest	the rest	
f (MHz)	433-2450	8500	10,000
ρ (kg·m^{-3})	1000	—	—
C (kJ·kg^{-1}·K^{-1})	3.60	3.53	3.53
κ (W·m^{-1}·K^{-1})	—	—	—
σ (S·m^{-1})	—	63.84 ± 3.73	66.88 ± 7.17
ε'_r	49-58	43.63 ± 0.82	40.90 ± 1.32
tan δ	0.33-1.70	0.32 ± 0.02	0.32 ± 0.03

[a]76.5% w/w saline solution containing 1.2% w/v salt was used.

Gel Phantoms for Thermal Therapy Experiments

In the following subsections, the various gel phantoms developed for hyperthermia and thermal ablation studies are reviewed. It is noteworthy that a number of phantom materials that are currently applied for imaging and diagnostic purposes (e.g., radiography, ultrasound, and magnetic resonance imaging) may also show potential for utilization in thermal therapy experiments. However, the present study aims to review the gel phantoms that have been specifically designed and developed for high-temperature experiments. In this section, the phantom materials are listed according to their introduction date, and thus the transposition does not show any precedence between these thermal phantoms.

TX-150 Phantoms

TX-150, widely referred to as "super stuff," is a gelling agent trademark sold by Oil Center Research Inc. (Lafayette, Louisiana). TX-150 is composed of approximately 33.5% w/w boric acid, 35.8% w/w guar gum, 22.9% w/w water, 6.7% w/w polyacrylamide, and 1.1 %w/w ester, probably triglyceride.[42] This material (and TX-151, the refined product) is currently used in radiology departments of hospitals and health facilities.

Phantom recipes. Table 2 presents two popular recipes proposed for simulation of high-water-content tissues (e.g., muscle and brain) at both LS-band (433-2450 MHz)[19] and X-band (8500 and 10,000 MHz)[43] frequency ranges. The thermal and electrical properties of these phantoms drastically depend on the gelling agent concentration. Therefore, a wide range of physical properties could be obtained by altering the TX-150 ratio. Table 3 also lists various formulas to simulate muscle at frequencies between 13.56 and 2450 MHz.[44] The dielectric constant of these phantoms is usually modified by addition of polyethylene powder and aluminum powder to the recipe, while NaCl is used to adjust the electrical conductivity of these phantoms.

Advantages and limitations. TX-150 phantoms could successfully mimic the high-water-content tissues (e.g., muscle and brain) in a wide frequency and temperature range. However, these gels are not suitable for simulation of tissues with low water content (bone and fat).[28] Moreover, TX-150 provides a variable gelation time, causing difficulties in standardization of gelation

Table 3. Composition (% w/w) of Muscle Phantoms Proposed by Chou et al. (1984) for Various Frequencies.[44]

f (MHz)	TX-150	Polyethylene	Al powder	NaCl	Water	σ (S·m^{-1})	ε_r'
2450	8.46	15.01	—	1.051	75.48	2.17 ± 0.08	47.4 ± 0.90
915	8.42	15.44	—	0.996	75.15	1.27 ± 0.02	51.1 ± 0.60
750	8.42	15.44	—	0.996	75.15	1.26 ± 0.04	52.5 ± 0.60
433	8.42	15.44	—	0.996	75.15	1.21 ± 0.01	53.5 ± 0.50
300	8.42	15.44	—	0.996	75.15	1.17 ± 0.01	54.8 ± 0.70
200	8.39	15.79	—	0.894	74.92	1.06 ± 0.02	56.7 ± 0.70
100	9.81	—	2.12	0.482	87.59	0.89 ± 0.01	71.5 ± 1.10
70	10.36	—	2.72	0.424	86.50	0.76 ± 0.01	84.7 ± 0.50
40.68	9.68	—	9.20	0.303	80.82	0.70 ± 0.02	97.9 ± 3.80
27.12	9.70	—	9.06	0.270	80.97	0.62 ± 0.02	113 ± 3.00
13.56	9.69	—	9.15	0.280	80.88	0.62 ± 0.03	149 ± 3.00

Reprinted with permission from Wiley.

parameters (e.g., temperature and mixing time).[44] The useful lifetime of TX-150 gels is also limited. A properly sealed phantom could be maintained for two weeks, and after this period, gel deterioration changes the phantom to a slurry with altered dielectric properties.

Agar Phantoms

Agar is a gelatinous polysaccharide derived from the cell membranes of some species of seaweed and red algae.[45] Due to the desirable physical and thermal properties, agar and agarose (the purified form) are widely used for fabrication of thermal phantoms. These phantoms are facilely fabricated by heating the agar aqueous solution above 85°C and then cooling the liquid to the room temperature, resulting in a lightly opaque gelatinous substance.[46]

Phantom recipes. One of the early researches concerning the development and characterization of the agar-based phantoms was carried out by Ishida and Kato (1980) for application at frequency of 13.56 MHz.[47] This recipe was later modified in further studies to reproduce the electrical properties of biological tissues at Industrial, Scientific, and Medical (ISM) frequencies including 435, 900, and 2450 MHz.[48,49] The composition and various properties of these phantoms are compared in Table 4. The agar phantoms are mainly consisted of agar as gelling agent and water. However, a number of components such as sodium azide (NaN_3)[48,50,51] or sodium dehydroacetate[49] as preservative, NaCl[47-50] or polyvinyl chloride (PVC)[51] as electrical conductivity modifier, and polyethylene powder[48] as dielectric constant regulator are usually added to these recipes. Note that the polyethylene powder could not be mixed directly in the agar solution and need be added with TX-151. The addition of NaN_3 may also result in a slight increase of electrical conductivity, while PVC powder could negatively affect the dielectric constant of agar phantoms.[50,51] Agar phantoms usually provide small permittivity values compared to the biological tissues, making these gels inappropriate for MW studies. This shortcoming could be overcome by adding some biological materials such as corn syrup.[52] However, these additives may increase the perishability of agar phantoms and lead to difficulties in controlling or reproducing the electrical properties. Graphite is another additive that is used for adjustment of both electrical conductivity and permittivity. The graphite powder could also produce "speckles" similar to those in biological tissues, resulting in more realistic ultrasound images.[53] However, graphite is only suitable for simulation of electrical conductivity and permittivity at MW frequencies.

Table 4. The Composition (% w/w) and Properties of Agar Phantoms Proposed for Radiofrequency and Microwave Studies.

				Ito et al. (2001)[48]		Takimoto et al. (2005)[49]
	Ishida and Kato (1980)[47]	Kato et al. (1986)[50]	Kato and Ishida (1987)[51]	Muscle	Brain	2/3 muscle[a]
Agar	2	4	4	2.70	2.50	2.30
NaCl	0.43	0-0.60	—	0.90	0.50	0.15
NaN_3	—	0.10	0-0.80	0.05	0.05	—
PVC	—	—	0-44.40	—	—	—
PE	—	—	—	8.60	13.30	22.30
TX-151	—	—	—	2.10	1.40	0.70
DASS	—	—	—	—	—	0.04
Water	the rest	the rest	the rest	the rest	the rest	the rest
f (MHz)	13.56	1-40	5-40	430	900	2000-10,000
T (°C)	22	23.50	23.60	22	22	—
ρ ($kg \cdot m^{-3}$)	—	1020	1020[b] (no PVC)	—	—	—
C ($kJ \cdot kg^{-1} \cdot K^{-1}$)	—	4.18	4.18 ± 0.08[b] (no PVC)	—	—	—
σ ($S \cdot m^{-1}$)	0.83	0.20-1.20	0.02-1.23	1.41	0.85	~0.60-7.50
ε_r'	109	~81	35-80	53	43	~27-36

PVC = Polyvinyl chloride; PE = Polyethylene powder; DASS = Dehydroacetic acid sodium salt.

[a]The target values were set to 2/3-muscle equivalent tissues, which correspond to the electrical constants of muscle equivalent tissues times 2/3.

[b]The density and specific heat capacity of PVC are 1380 $kg \cdot m^{-3}$ and 1298 $J \cdot kg^{-1} \cdot K^{-1}$; Therefore, the ρ and C values of the final phantom can be calculated from the proportion of PVC in the phantom.

Agar-based phantoms have also been applied for HIFU experiments. The majority of these HIFU phantoms are developed according to a recipe proposed for diagnostic ultrasound application.[54] This recipe is composed of water, agar, graphite powder as scatterer, methyl paraben as preservative, and 1-propanol as sound speed modifier. This recipe exhibits a thermal conductivity in the range of biological tissues. However, the attenuation coefficient of this phantom at 1 MHz is slightly higher than that of soft tissues, causing higher peak temperatures and smaller heated volumes in the phantoms compared to real tissues.[55] The attenuation coefficient could be moderated by lowering the ratio of graphite powder in the recipe.[46,56] Nylon threads are also suitable acoustic scatterers due to their high durability and oxidation resistance.[13] Calcium,[45] magnesium,[45] potassium,[45] sawdust,[45] glycerol,[57] cellulose,[57] evaporated milk,[58] glass beads,[3,58] silicon dioxide, and silicon carbide[59] are other materials that could be used as ultrasound attenuating agents. On the contrary, thiomersal[58] or formaldehyde[60] could replace methyl paraben to protect the gel against deterioration. Formaldehyde also cross-links the gel molecules, which consequently decreases the compliance and increases the melting point of agar phantoms.[60] It is important to note that the inertial cavitation threshold reported for the agar-based phantoms is significantly lower than that of biological tissues which thus results in a considerably higher bubble-enhanced heating during HIFU sonication.[55,56] However, well-degassed agar phantoms containing increased ratios of gelling agent may provide improved P_{cav} values. The various properties of some popular recipes developed for HIFU experiments are summarized in Table 5.

The optothermal properties of agar-based phantoms have also been characterized. Pure agar gel exhibits a very low turbidity and a negligible absorption. Therefore, its optical properties could easily be adjusted by adding appropriate scattering (e.g., intralipid,[61] vasolipid,[62] and evaporated milk[62]) and absorbing (e.g., India ink,[61] indocyanine green,[62] and naphthol green[63,64]) agents. The ability of agar gels to be quickly scanned under magnetic resonance imaging system

Table 5. The Composition and Properties of Agar-Based Phantoms Developed for High Intensity Focused Ultrasound Experiments.

	Holt and Roy (2001)[55a]	Huang (2004)[46]	Farny et al. (2010)[56]	Ortega et al. (2010)[13]	
Agar	2.50	2.50	2.70	2.50	3
Graphite powder	9.00	7.60	3.70	100 ($g \cdot L^{-1}$)	—
Nylon	—	—	—	—	Threads[b]
1-propanol	5.30	5.60	1.90	—	—
Glycerol	—	—	—	5	5
Preservative	0.10	0.10	0.10	—	—
Water	the rest	the rest	the rest	the rest	the rest
f (MHz)	1	1	1	3.50	3.50
T (°C)					
ρ ($kg \cdot m^{-1}$)	1100 ± 50	1045	1003	—	—
C ($kJ \cdot kg^{-1} \cdot K^{-1}$)	3.30 ± 0.50	3.71	3.71	—	—
κ ($W \cdot m^{-1} \cdot K^{-1}$)	0.65	0.59	—	—	—
D ($mm \cdot s^{-1}$)	—	—	0.158	—	—
α ($dB \cdot cm^{-1} \cdot MHz^{-1}$)	1.60 ± 0.1	0.88	0.44	0.31-0.68	0.48-0.62
c ($m \cdot s^{-1}$)	1600 ± 25	1551	1520	1519-1560	1601-1645
P_{cav} (MPa)	~1.42[c]	—	1.40[d]	—	—

The amounts of ingredients are presented in % w/w, unless otherwise specifically stated.
[a]This phantom was made using 600 mL of water, 750 mg of methyl paraben, 18 g of agar, 65 g of graphite powder, and 48 mL of 1-propanol. These values are converted to %w/w in this table.
[b]Nylon threads formed a matrix of 7 × 7 parallel units, by regular distance of 5 mm between them.
[c]The pulse repetition frequency (PRF) was not reported. Various sonication durations between 0.7 s and 10.2 s were used. However, it was found that the P_{cav} value was constant at sonication durations above 1 s.
[d]The sonication duration was fixed at 5.5 s.

(MRI) is an attractive incentive for clinical application.[64] Moreover, by incorporation of thermo-responsive proteins such as albumen (a condensed form of egg-white)[63] and Bovine Serum Albumin (BSA),[64] heat-sensitive agar phantoms suitable for photocoagulation studies could be obtained. When these phantoms are heated at temperatures above 70°C, the added proteins undergo an irreversible coagulation that changes the optical and MR values of the gel, allowing to distinguish the heated region inside the phantom. However, a trade-off exists between tissue equivalency and heat-sensitivity by considering that the addition of scatterers such as intralipid could suppress the digital response from the coagulated protein, and thereby decrease the heat-sensitivity of these gels.[64]

Heterogeneous agar-based phantoms. Agar-based gels are promising candidates for the construction of heterogeneous phantoms that simulate inner tumors surrounded by background tissue.[65] Tumor-tissue phantoms are mostly constructed by solidifying two solutions containing different ratios of agar. In a typical recipe, a solution containing 0.25% w/w agar, 3% w/w sucrose, and designated ratios of NaCl (0.3%-36.0% w/w) is used to form the tumor-mimicking compartment. The tissue-mimicking part is also fabricated by solidifying an aqueous solution consisting of 5% w/w agar, 3% w/w sucrose, and different concentrations of NaCl (0.06%-5.00 % w/w).[65] Designated amounts of fat-saturated oil could be added to the outer compartment to reduce the thermal conductivity of this layer, causing a more heat deposition within the central tumor.[66] The thermal conductivity of the outer part could be tuned in the range of 0.48 (normal liver) to 0.23 $W \cdot m^{-1} \cdot K^{-1}$ (fat) by varying the concentration of the fat-saturated oil (10%-90%).[66] Ortega-Palacios et al.

(2010) also proposed a tumor-breast phantom for MW ablation of breast cancer.[67] The breast compartment composed of agarose, corn oil, and a neutral detergent, while the tumor part contained agarose, ethanol, and NaCl. Measurement of the dielectric properties of this phantom in frequency ranging 2 to 3 GHz showed that the applied frequency could result in a positive impact on electrical conductivities and a negative influence on dielectric constants of both layers. However, the impact of frequency on dielectric properties of tumor part was more significant than that of breast compartment.[67]

Due to the desirable mechanical strength, agar-based gels could be used for the construction of tissue-mimicking phantoms that simulate the vascular system, surrounding tissue, and blood. These phantoms are typically composed of a latex or silicon rubber tube, which represents the blood vessels surrounded by a tissue-mimicking gel.[45] In particular, the relatively high stiffness of agar gels allows the implementation of wall-less vessel phantoms to avoid the difficulties associated with vessel wall attenuation and acoustic impedance mismatches.[57] The wall-less vessel simulant is usually formed by placing a metallic mandrel into the solution prior to gelation and removing it after hardening.[57] An alternative method for construction of more complicated vessel geometries (e.g., Y-shaped vessels) is the use of low-melting-point cores, which are further removed from the structure by submersion of the solidified agar phantom in a water-bath at mild temperatures (approximately 50°C).[60]

Advantages and limitations. The high melting point of agar phantoms (approximately 80°C) is desirable for applications where high-temperature regimes are achieved.[13] Moreover, agar phantoms exhibit a sufficient mechanical strength that permits the construction of large torsos.[50] The critical properties of these phantoms can easily and independently be varied by altering the ratios of phantom ingredients. In particular, the sound speed can be adjusted by varying the percentage of 1-propanol, while the attenuation is controlled by adding graphite powder. However, optical opacity is the crucial limitation of agar phantoms, causing difficulties in visual observation of the coagulated region.[46] The agar phantoms also provide a low toughness, making them fragile during handling.

Acrylamide Phantoms

Acrylamide-based polymers are the most popular materials utilized for the fabrication of thermal phantoms. Polyacrylamide (PAA) phantoms are fabricated by cross-linking of acrylamide monomer (AA) using N,N'-methylene-bis-acrylamide (MBAA) in aqueous solutions at room temperature in the presence of an initiator usually ammonium persulfate (AMPS) and tetrametyl-ethylene-diamine (TEMED).[64]

Phantom recipes. The PAA phantoms are widely used for simulation of human body in both RF and MW frequency ranges.[10,68,69] The composition and various properties of the most popular recipes used for construction of RF/MW PAA phantoms are shown in Table 6. The dielectric properties of these phantoms drastically depend on the type and ratio of the gel constituents. For instance, to simulate a low-conductivity tissue, the NaCl content need be reduced. Lower levels of conductivity are also obtained by reducing the AMPS ratio. In fact, AMPS could be removed and the reaction is initiated by increasing the temperature near the melting point of acrylamide. Decreased permittivity values could be obtained using nonpolar or low-permittivity liquids (e.g., dioxane, pyridine, and ethylene glycol) instead of water. The AA concentration also shows a negative correlation with both electrical conductivity and relative permittivity as well as a positive correlation with mechanical strength.[10] For application in HIFU experiments, the acoustic attenuation of PAA gels could be adjusted using evaporated milk, intralipid[70] (or glycerol[24] for

Table 6. The Ingredients and Properties of Different Suggested Polyacrylamide-Based Phantoms.

	Bini et al. (1984)[10]			Surowiec et al. (1992)[69]	
	High-Water	Low-Water	Andreuccetti et al. (1988)[68]	Muscle	Lung
Acrylamide	15	40	27-32	26 (% w/w)	28 (% w/w)
MBAA	0.10	~0.27	0.18-0.21	0.196 (% w/w)	0.22 (% w/w)
TEMED	~0.39(0.5 mL)	~1.03(1.33 mL)	0.70-0.82	0.05 (% w/w)	0.05 (% w/w)
AMPS	0.13	0.07	0.13	1 (% w/w)	0.75 (% w/w)
NaCl	0.50[a]	0.58	0-1.75	1.05 (% w/w)	0.433 (%w/w)
Glycerin	—	—	—	—	15 (% w/w)
Water	the rest	—	the rest	the rest	the rest
Ethylene glycol	—	the rest	—	—	—
f (MHz)	27[a]	27	750-5500	500-3000	500-3000
T (°C)	20[a]	20	20	37	37
ρ (kg·m^{-3})	1030	~1000	—	1070	—
C (kJ·kg^{-1}·K^{-1})	4.18	~4.18	—	3.47	—
κ (W·m^{-1}·K^{-1})	0.41	0.23	~0.40	0.40 0.56[b]	—
σ (S·m^{-1})	0.61	0.01	—	—	—
ε_r'	—	21.80	44.50-52	63	38
ε_r''	—	—	14.50-36.30	65	33

The amounts of ingredients are presented in % w/v, unless otherwise specifically stated.
MBAA = N,N'-methylene-bis-acrylamide; TEMED = tetra-metyl-ethylene-diamine; AMPS = ammonium persulfate.
[a]The authors proposed a formula to determine the needed NaCl based on temperature (20-40°C) and frequency (13.56-40 MHz). However, for brevity, only the base recipe for T = 20°C and f = 27 MHz are presented here.
[b]Data were reported by Davidson and Sherar (2003).[8]

enhanced transparency level), and corn syrup.[70,71] The optothermal properties of PAA gels could also be adjusted by incorporation of appropriate additives such as bovine hemoglobin (optical absorber), polyvinyl acetate (PVA, scattering particles), magnevist (T_1 contrast agent), and lumirem (T_2 contrast agent), to simulate biological tissues in laser studies.[72]

Heat-sensitive acrylamide-based phantoms. The most crucial characteristic of PAA gels is their transparency in optical range, enabling visualization of the coagulation zone inside the phantoms by adding some heat-sensitive ingredients including BSA, egg-white, non-ionic surface active agents, and thermochromic dyes.

BSA is a popular heat-sensitive protein, which is widely used to capture the heat damage inside the phantoms.[73] The thermal coagulation of BSA at temperatures between 60°C and 70°C forms a white and opaque lesion in the phantom that represents the region where the temperature exceeded this threshold point. The thermal lesion also results in a reduced T_2 value that provides a contrast for observation of the heated region in T_2-weighted MR images. These phantoms could be applied to determine bubble activity during HIFU experiments. The gradual heating because of pure thermal effects results in a cigar-shaped lesion (Figure 1(a)) in PAA-BSA phantoms, while a combination of thermal and cavitational effects produces tadpole-shaped or egg-shaped lesions (Figure 1(b) & 1(c)).[74] The PAA-BSA phantoms provide an inertial cavitation threshold within a range similar to that of biological tissues (7-10 MPa).[75-77] The acoustic absorption and scattering of PAA-BSA phantoms could be adjusted in the range of target tissues using evaporated milk, corn syrup, intralipid,[70] or glass beads.[78] However, the

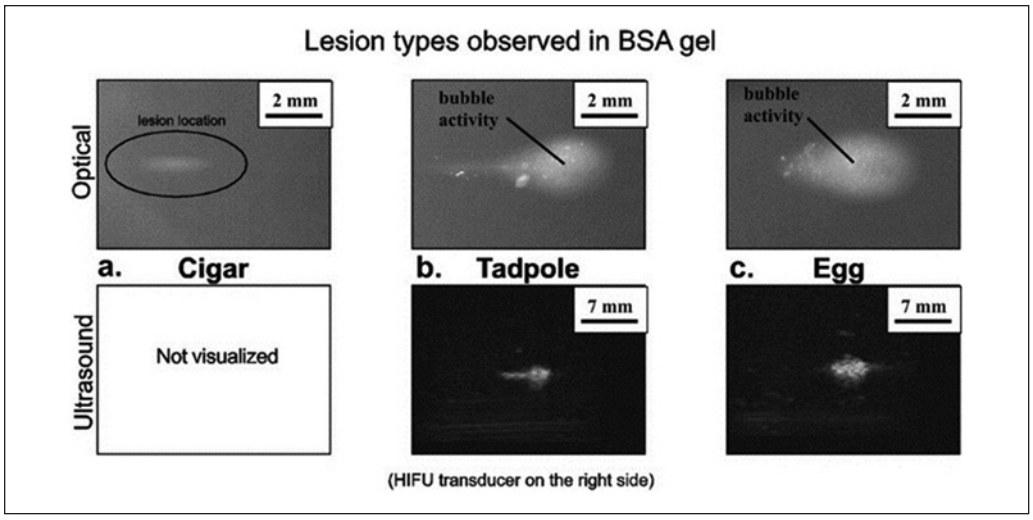

Figure 1. Thermal lesions produced in a PAA phantom containing 6% BSA and their corresponding ultrasound images (if observation occurred): (a) cigar-shaped, (b) tadpole-shaped, and (c) egg-shaped lesions.[74] Reprinted with permission from Elsevier. PAA = Polyacrylamide; BSA = Bovine Serum Albumin; HIFU = High Intensity Focused Ultrasound.

coagulation temperature of these heat-sensitive phantoms (approximately 60-70°C) is relatively higher than that of biological tissues, resulting in an inaccurate simulation of tissue coagulation during thermal therapies. The coagulation temperature could be lowered to 50°C by decreasing the pH from 4.7 to 4.3 using citrate buffer.[70] The pH level also shows a positive impact on specific heat capacity of the phantoms.[24] Another significant drawback of PAA-BSA phantoms is their low attenuation coefficient, which could be eight times smaller than that of real tissues.[74,79] Although the PAA-BSA phantoms are mostly used for HIFU experiment, their composition could be modified to present suitable dielectric properties for RF application.[24] The concentrations of AA and MBAA in RF phantoms must be higher compared to HIFU phantoms, enabling the gels to be hard enough for standing on the dispersive ground pad and tolerating insertion of electrodes without cracking. The composition and various properties of PAA-BSA phantoms are summarized in Table 7.

Egg-white (EW) is another protein that is widely applied in construction of heat-sensitive phantoms for HIFU experiments.[80] When a PAA-EW phantom is sonicated using HIFU beams, the EW protein in the focal point is heated and consequently coagulated (Figure 2). Using EW as a heat-sensitive agent in the PAA phantoms results in similar benefits for lesion visualization as BSA, yet incurring a lower cost. An investigation on the influence of EW concentration on the acoustic properties of PAA phantoms demonstrated its positive impact on both sound speed and attenuation coefficient. The attenuation coefficient could be adjusted between 0.1 and 1.3 $dB \cdot cm^{-1}$ by varying the EW concentration.[80] Because of its high water content, EW could be used in construction of PAA-based heat-sensitive phantoms without using additional water.[6] Table 8 presents the composition and various properties of the PAA-EW phantoms developed in previous studies. The sound speed and attenuation coefficient of these phantoms exhibit positive and negative relationships with temperature rise, respectively. Studies also show an increased attenuation coefficient in the coagulated zone compared to the surrounding region. However, the sound speed in the coagulated zone remains almost identical to that of non-coagulated material at constant temperatures.[6]

Table 7. The Composition (% w/v) and Various Properties of Polyacrylamide-Based Phantoms Containing Non-Ionic Surface Active Agents Developed by Researchers.

	Lafon et al. (2001)[79]	McDonald et al. (2004)[70]	Bu-Lin et al. (2008)[24a]
Acrylamide	7	7	9.50
MBAA	—	0.14	0.50
BSA	3-9	2	2 (lyophilized powder)
Initiators			
TEMED	~0.05[b]	—	—
AMPS	~0.07[b]	—	—
Ascorbic acid	—	0.01	0.01
Ferrous sulfate	—	0.0025	0.0025
H_2O_2	—	0.03	0.03
pH modifiers			
CAA	—	1.91	—
CAM	—	—	2.49
SCT	—	2.96	2.40
Sound absorber			
Intralipid	—	6	—
Glycerol	—	—	~75 (60 mL)
Water	the rest	the rest	the rest
f (MHz)	1-5	5	0.47
T (°C)	22	—	37
ρ (kg·m^{-3})	1044	—	1069 ± 3
T_C (°C)	>70	50-60	50-60
C (kJ·kg^{-1}·K^{-1})	~5.1	—	3.68 ± 0.20
κ (W·m^{-1}·K^{-1})	0.70	—	—
D (m^2·s^{-1})	1.3 × 10^{-7}[c]	—	—
α (dB·cm^{-1}·MHz^{-1})	~0.08-0.18	0.52 ± 0.03	—
c (m·s^{-1})	1544	1556 ± 4	—
Z (Mrayl)	1.61	—	—
B/A	4.8-5.1[d]	—	—
P_{cav} (MPa)	~6[e] 8.67 ± 0.44[f,g] 0.94 ± 0.13[f,h]	—	—
σ (S·m^{-1})	—	—	~0.12

MBAA = N,N'-methylene-bis-acrylamide; BSA = Bovine Serum Albumin; TEMED = tetra-metyl-ethylene-diamine; AMPS = ammonium persulfate; CAA = citric acid anhydrate; CAM = citric acid monohydrate; SCT = sodium citrate tribasic dehydrate.

[a]The authors examined the electrical properties of phantoms in three different pH phantoms (4.3, 4.5, and 4.7). However, for brevity, only the data for the recipe with pH of 4.3 are presented in this table.

[b]0.01 mL TEMED per 15 mL Liqui-gel and 0.05 mL of 10% AMPS solution per 15 mL Liqui-gel were used.

[c]Data are presented by Canney et al. (2010) for BSA ratio of 7% w/v at f = 2.158 MHz.[16]

[d]The nonlinearity coefficient was measured by Lafon et al. (2005).[74]

[e]The P_{cav} value was measured by Khokhlova et al. (2006) using a 200-cycle burst at f = 2 MHz (7% w/v BSA).[77] The sonication duration and PRF were 4 s and 1 KHz, respectively.

[f]The values are reported by Zhang and Porter (2010) using a 80-cycle pulse at f = 2 MHz (7% w/v BSA).[76]

[g]The recipe contains 0.3% v/v albumin-coated dodecafluoropentane.

[h]Phantom contains 0.8% v/v 2H, 3H-perfluoropentane.

The crucial limitation of BSA and EW is their permanent coagulation process. Therefore, the phantom containing BSA or EW cannot be reused and need to be discarded after

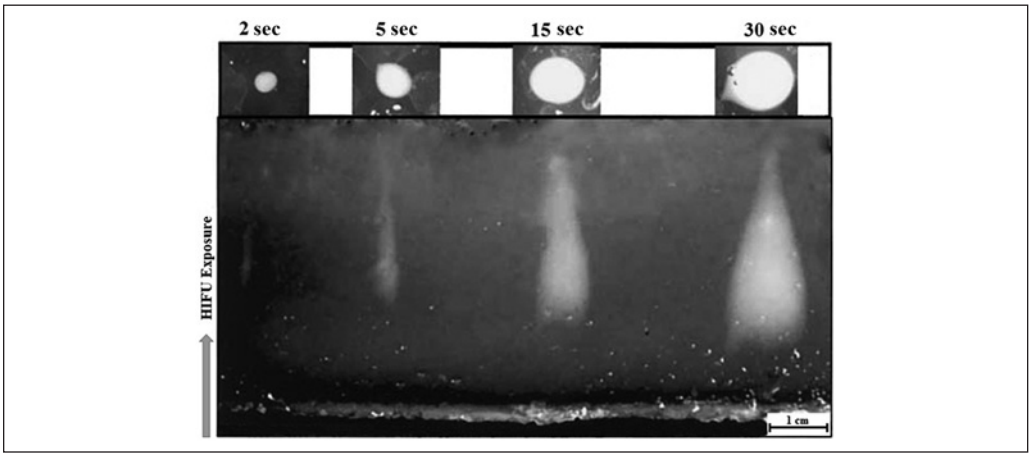

Figure 2. Polyacrylamide phantom containing 30% egg-white sonicated with HIFU beams for 2, 5, 15, and 30 s. The cross and axial views of the coagulated lesion are shown at the top and the bottom, respectively.[80] Reprinted with permission from Elsevier. HIFU = High Intensity Focused Ultrasound.

Table 8. Various Polyacrylamide-Egg-White Recipes Suggested in the Literature.

	Takegami et al. (2004)[80]	Divkovic et al. (2007)[6]	Labuda and Church (2011)[15]
Acrylamide + MBAA[a]	24.80	~12.50	25
TEMED	0.20	~0.20	0.20
AMPS[b]	0.50	~0.50	0.50
Egg-white	0-40	the rest	30
Water	the rest	—	the rest
f (MHz)	1.10-5.56	1-3	5
T (°C)	25	26-55	25
ρ (kg·m^{-3})	990-1000	1045 ± 5	—
T_C (°C)	—	67	60
C (kJ·kg^{-1}·K^{-1})	—	4.27 ± 0.37	4.27
κ (W·m^{-1}·K^{-1})	—	0.59 ± 0.06	0.59
α (dB·cm^{-1}·MHz^{-1})	0.14-1.29	0.14-0.67	1.04
c (m·s^{-1})	1537-1544	1546 ± 31	1541
Z (Mrayl)	—	—	1.50

The ratios are presented in % v/v. MBAA = N,N'-methylene-bis-acrylamide; TEMED = tetra-metyl-ethylene-diamine; AMPS = ammonium persulfate.

[a]An aqueous solution containing 38% w/w acrylamide and 2% w/w bis-acrylamide was used.

[b]A solution of 10% w/w AMPS was used.

coagulation occurs. To overcome this matter, non-ionic surface active agents (NISAAs) have been proposed as alternatives for BSA and EW in constructing reusable thermal phantoms. NISAAs are a group of material that undergoes segregation when temperature exceeds a specific degree called "the clouding point (T_{CP})," resulting in a white and opaque region. These materials return to their original transparency when cooled again below their clouding point. Several categories of NISAAs have been developed with different clouding points including polyoxyethylene-polypropylene condensates, polyoxyethylene-polypropylene condensates of

Table 9. The Composition and Properties of Polyacrylamide Thermal Phantoms Containing Non-Ionic Surface Active Agents.

	Miyakawa et al. (1995)[81]	Miyakawa et al. (1998)[82]		Park et al. (2010)[71]
Acrylamide + MBAA	3[a]	3[a]	13[a]	7.50 (v/v)[b]
TEMED	0.02-0.50[c]	0.02-0.50[c]	0.02-0.50[c]	0.05 (% v/v)
AMPS	0.03-0.14[c]	0.03-0.14[c]	0.03-0.14[c]	~0.80 (% v/v)
NISAA	1	1	0.5	5 (% w/v)
NaCl	0.29-0.83	2.5	2.5	—
Butanol	—	0.5	—	—
Sucrose	—	—	24	—
Corn syrup	—	—	—	40 (% w/v)
Water	the rest	the rest	the rest	58 (% v/v)
f (MHz)	27-860	430	850	1-5
T (°C)	25	25	25	25
ρ (kg·m^{-3})	—	1020	—	—
T_{CP} (°C)	30.70-31.60	30.10	18	48-57 (onset) 65-74(ending)
C (kJ·kg^{-1}·K^{-1})	—	4.25	—	—
κ (W·m^{-1}·K^{-1})	—	6.45 × 103	—	—
α (dB·cm^{-1}·MHz^{-1})	—	—	—	0.40 ± 0.05
c (m·s^{-1})	—	—	—	1568-1573
Z (Mrayl)	—	—	—	1.64-1.66
σ (S·m^{-1})	—	1.21	1.69	—
ε_r'	72.50-79.80	73.50	51.60	—

Data are reported in % w/w, unless otherwise specifically stated.
MBAA = N,N'-methylene-bis-acrylamide; TEMED = tetra-metyl-ethylene-diamine; AMPS = ammonium persulfate; NISAA = non-ionic surface active agent.
[a]Containing 2% MBAA.
[b]An aqueous solution containing 38% w/w acrylamide and 2% w/w bis-acrylamide was used.
[c]The concentration varies according to the room temperature.

ethylenediamine, second-class chained alcohol-ethoxylates, nonylphenol-ethoxylates, octhylphenol-ethoxylates, polyoxyethylene-cetylethers, and polyoxyethylene-alkylethers.[81] In general, T_{CP} depends on the NISAA type and ratio, the concentration of gelling and cross-linking agents, ratio of the ionization material (e.g., NaCl), and the presence of some alcoholic compounds such as methanol, ethanol, 1-propanol (as T_{CP} boosters), and n-butanol (as T_{CP} moderator).[71,81] T_{CP} is also affected by the pH level of solution as well as the type of buffer used. In particular, acetate and tromethamine buffers show weaker suppression of T_{CP} than citrate and phosphate buffers.[71] Various types of NISAAs with different clouding points ranging from 20°C to above 100°C have been examined to construct heat-sensitive phantoms in RF/MW[81,82] and HIFU[71] experiments (Table 9). The physical properties of the PAA phantoms may slightly be affected by adding NISAAs. For instance, the addition of NISAAs from polyoxyethylene-alkylether category results in small increases in both sound speed and acoustic impedance values, while the attenuation coefficients and densities remain almost constant.[71] However, a significant drawback of NISAAs is a wide gap between the onset and ending temperatures of clouding. Using a NISAA from the polyoxyethylene-alkylether category could result in a 17°C and 20°C difference between the onset and ending temperatures of clouding and clearing processes, respectively. Moreover, the onset temperature of clearing is approximately 5°C lower

than the ending temperature of clouding.[71] These results show the inability of NISAAs in precise estimation of temperature rise inside the phantom.

Reusable heat-sensitive PAA phantoms could also be fabricated using thermochromic dyes.[83] These dyes are usually colored below a threshold temperature and change to colorless at higher temperatures. Thermochromic dyes provide reversible heat-sensitivity with more precise threshold temperatures compared with BSA, EW, and NISAAs (approximately ± 3°C). Furthermore, due to the low ratio of dye needed for preparation of heat-sensitive phantoms, most thermal and acoustic properties of these phantoms remain identical to those of reference phantom (phantom without dye). However, the transparency level of PAA phantoms is significantly reduced after addition of these heat-sensitive agents. Therefore, thermochromic dyes are only useful for fabrication of phantoms with dimensions smaller than 10 cm.[83]

Due to their suitable mechanical properties, PAA-based gels also allow the construction of heat-sensitive vasculature-mimicking phantoms.[84] In these phantoms, a thin-wall vessel compartment is produced using a thermal-sensitive powder and silicon-based gel. Due to the optical transparency of the surrounding PAA gel, the temperature changes of the vessel-mimicking component could be visually observed during HIFU sonication.

Advantages and limitations. Acrylamide is the most widely used gelling agent for construction of heat-sensitive phantoms, especially for HIFU application. These gels exhibit high melting points that provide a sufficient stability in thermal therapy experiments.[64] The optical transparency, formability into complex forms, gel-like mechanical properties, and the ability to represent a wide range of thermal, electrical, and acoustic properties are other attractive properties that make these gels promising candidates for simulation of both high-water-content and low-permittivity low-conductivity tissues (bone and fat).[28]

In general, toxicity of the ingredients is the most critical limitation of the PAA-based phantoms. Acrylamide monomer is a severe neurotoxin that requires extreme precautionary measures during the fabrication process. These phantoms also show a limited shelf life—from several hours when exposed to air to few weeks when kept in an airtight container.[10] The polymerization of acrylamide is an exothermic reaction, causing a rapid temperature rise shortly after mixing the solutions. This temperature rise may consequently cause an undesired coagulation of the heat-sensitive proteins during the phantom preparation. Furthermore, due to a rapid polymerization reaction, a short time period (about 30 s) is available for stirring, casting, and degassing the unpolymerized solution. Continuous cooling of the mixture prior to polymerization may increase the available time for stirring and degassing of the solution.

Hydroxyethyl Cellulose Phantoms

Hydroxyethyl cellulose (HEC) is a gelling agent derived from cellulose and primarily used as thickening material in ophthalmic and topical formulations. HEC is also used with hydrophobic drugs in capsule formulations to improve drug dissolution in the gastrointestinal fluids.[85]

Phantom recipes. HEC-based phantoms were first developed by Hartsgrove et al. (1987) for electromagnetic dosimetry and hyperthermia applications.[86] This phantom was later used to simulate human brain tissue at 835[21] and 900[29] as well as liver tissue at 915 MHz[87] and 2450 MHz.[5] A typical HEC-based phantom consists of water, HEC, NaCl/sugar (to increase and reduce the electrical conductivity, respectively), and a preservative. By using preservative and prevention of water evaporation, the phantom can be protected for nearly one year. Table 10 lists the composition and various properties of the HEC-based phantoms developed in previous studies.

Table 10. The Composition and Different Properties of Hydroxyethyl Cellulose Thermal Phantoms.

	Faraone et al. (1998)[21]	Stauffer et al. (2003)[87]		Ozen and Koylu (2005)[29]
HEC	1	2.05		0.90
Sugar	56	46.01		54.66
NaCl	2.50	0.82		0.72
Bactericide	0.20	0.10		0.17
Water	40.30	51.02		43.55
f (MHz)	835	915	2450	900
ρ (kg·m^{-3})	—	1160[a]	1160[a]	—
C (kJ·kg^{-1}·K^{-1})	—	3.05[a]	—	—
σ (S·m^{-1})	0.90	0.96 1.0[a]	2.74[a]	0.92
ε_r'	44	51.30 51.90[a]	42.70[a]	44

The amounts of ingredients are reported in % w/w. HEC = Hydroxyethyl cellulose
[a]Data are presented by Prakash et al. (2006).[5]

Advantages and limitations. HEC-based phantoms are promising candidates for serial studies due to their long-term stability and facile fabrication procedure. However, more studies are needed to characterize the thermal stability as well as the acoustic and optical properties of these phantoms.

Gelatin Phantoms

Gelatin is a mixture of peptides and proteins produced by physical, thermal, or chemical degradation of collagen extracted from the skin, tendon, cartilage, bone, and some intestines of animals. Gelatin is widely used as a gelling agent in the medical and pharmaceutical fields due to its biocompatibility, bio-degradability, non-immunogenicity, biological origin, and commercial availability at low cost.[88-90] The gelation process of this material that occurs at temperatures below 40°C is due to a conformational disorder–order transition of the gelatin chains that form thermoreversible networks by associating helices in junction zones stabilized by hydrogen bonds.[89]

Phantom recipes. The first gelatin-based thermal phantom was developed to simulate the dielectric properties of human muscle at low frequency ranges.[91] This gel was composed of 20% gelatin with electrical conductivity of 0.27 to 0.48 S·m^{-1} and relative permittivity of 90 to 93 at 27 MHz and temperature range of 15°C to 50°C.[91] The examination of dielectric constant and electrical conductivity of this phantom in frequency range of 10 to 150 MHz showed the positive and negative impacts of applied frequency on electrical conductivity and dielectric constant, respectively.[92] Therefore, by variation of the ε_r' frequency, the and σ values were altered in the ranges of 40 to 115 and 0.14 to 0.65 S·m^{-1}, respectively.[92] Due to their appropriate dielectric (ε_r' and ε_r''), thermal (C and k), and physical (ρ) properties, the gelatin-based phantoms are suitable for simulation of both high-water (muscle) and low-water (fat) tissues at different frequency ranges (Table 11).[26,93]

Heterogeneous gelatin phantoms. A crucial advantage of gelatins is their ability to fabricate heterogeneous structures with long-term stability of physical and mechanical properties.[94].Based on

Table 11. The Ingredients and Various Characteristics of Gelatin-Based Phantoms.

	Robinson et al. (1991)[26]			Yuan et al. (2012)[93]		
	Muscle	Fat	Sunaga et al. (2003)[97]	Tumor[a]	Muscle[a]	Fat[a,b]
Gelatin	10	5	13.50	95 (% v/v)[c]	90 (% v/v)[c]	15 (% v/v)[c]
Oil				5 (% v/v)	10 (% v/v)	85 (% v/v)
NaCl	2	—	1.70	0.75 (% w/v)	0.60 (% w/v)	0.024 (% w/v)
Polyethylene	—	40[d]	—	—	—	—
Honey	—	—	50.10	—	—	—
Ethanediol	48	55	—	—	—	—
Water	the rest	—	the rest	—	—	—
f (MHz)	50-2450	50-2450	64-400	100-433	100-433	100-433
T (°C)	20	20	20	37	37	37
ρ (kg·m^{-3})	1100	950	—	—	—	—
C (kJ·kg^{-1}·K^{-1})	3.70	2.25	—	3.71	3.48	2.-17
κ (W·m^{-1}·K^{-1})	0.43	0.29	—	0.49	0.42	0.20
σ (S·m^{-1})	—	—	0.41-0.66	0.844-0.969	0.641-0.759	0.019-0.034
ε_r'	39.50-53.60	6.00-11.40	49.50-56.30	61.52-69.38	55.30-6147	6.78-7.66
ε_r''	22.50-33.50	3.50-3.60	—	—	—	—

The concentration of ingredients are presented in % w/w, unless otherwise specifically stated.
[a]The solution contains a small amount of surfactant to decrease the surface tension between the oil and water.
[b]The fat and the bone marrow materials had same composition since their dielectric properties were very similar in the studied frequency range.
[c]An aqueous gelatin solution was used in this recipe.
[d]A drop of detergent was also added to help wet the polythene powder, which is then stirred in.

this fact, stable heterogeneous breast phantoms for ultra-wide band frequencies (0.5-20 GHz) have been developed.[28] The dielectric properties of this phantom were adjusted using a varying ratio of oil (a solution of 50% kerosene and 50% safflower oil). In this recipe, a component containing 10% oil was made to represent the hepatic tissue at both 915 and 2450 MHz, whereas the gels containing 80% and 10% oil were produced for mimicking the breast fat and cancerous lesions at frequency range of 1 to 11 GHz, respectively.[28]

The geometrical, thermal, and dielectric properties of human thigh with fat, muscle, and deep-seated tumor could also be simulated using heterogeneous gelatin phantoms.[93] To achieve this, the mixture of kerosene and safflower oil must be substituted by pure canola oil due to the closer thermal and MR properties of canola oil to human fat. A few drops of a surfactant also need to be added to decrease the surface tension between the canola oil and water. The electrical conductivity of this heterogeneous structure at frequency ranges below 1 GHz could be tuned by adding NaCl. At higher frequencies, due to a significant increase in water conductivity, both dielectric constant and electrical conductivity must be adjusted by increasing the oil ratio. The composition and various properties of these heterogeneous phantoms at various frequency and temperature ranges are summarized in Table 11.

Because of suitable optical properties, the gelatin phantoms are also applicable in construction of heterogeneous tumor-tissue structures for optothermal studies. The normal tissue is simulated using gelatin and Liposyn II intralipid, while the tumor-mimicking sphere is prepared using the same recipe with designated ratios of indocyanine green. The indocyanine green results in a higher absorption coefficient, and consequently, increased energy storage within the

tumor-mimicking region. Similarly, gelatin has been used in construction of prostate phantoms incorporating tumor, rectum, and urethra for laser ablation studies.[95]

Advantages and limitations. The long-term stability, low cost, and facile production of gelatin-based phantoms make these materials suitable for serial studies. Despite the base phantoms are easily fabricated by mixing of gelatin in aqueous solutions, various additives including acrylamide/MBAA as coagulant,[96] ethanediol and polyethylene powder as modifiers of electrical properties,[26] honey syrup as preservative,[97] glutaraldehyde as gelation accelerator,[94] and graphite powder as controller of acoustic properties[98] could be used to modify the physical and mechanical properties of these gels. On the contrary, the main limitation of gelatin phantoms is their low mechanical strength as well as low melting temperature that makes them impractical for application in temperature regimes above 50°C. Although both thermal and mechanical stability of these phantoms could be improved by adding formaldehyde as a cross-linking agent,[28] the resultant phantoms may not provide favorable thermal and mechanical properties compared with acrylamide or agar phantoms.

Gellan Gum Phantoms

Gellan gum is an extracellular polysaccharide secreted by the microorganism Sphingomonas elodea and possesses a linear structure with repeating units of tetrasaccharide. The gellan gum gels are formed due to a disorder–order coil-helix transition that occurs during the cooling of the heated gellan gum solutions in the presence of gel-promoting cations such as sodium, potassium, calcium, and magnesium.[99,100]

Phantom recipes. The gellan gum phantoms were first developed by Miyakawa et al. (1995) for electromagnetic studies.[81] The fabricated phantom exhibited sufficient transparency, which thus provided the ability to visualize the heated region by adding NISAAs to the phantom recipe. This recipe was later modified for HIFU application by adding aluminum oxide particles as scatterers to adjust the attenuation and backscatter, as well as 1-propanol to control the sound speed. Calcium chloride dehydrate was also used to enhance the gel strength, while potassium sorbate acted as preservative.[101] Specific ingredients used in both recipes are listed in Table 12.

Advantages and limitations. Gellan gum is an attractive material as it forms a gel at low concentrations (as low as 0.01% w/w) and provides a sufficient transparency for visualization of the coagulation region inside the phantoms.[100] Moreover, due to their stability at high-temperature regimes (about 95°C), the gellan gum phantoms are applicable in thermal ablation studies. Gellan gum also presents a very homogeneous structure, resulting in suitable ultrasound images. In the cases where a less homogeneity degree is required, designated amounts of alumina powder (with particle sizes of 0.8-1.5 mm) could be added to the base phantom. However, the main drawback of these phantoms is the strong dependence of their acoustic and thermal properties on the construction protocol, which causes difficulties in achieving reproducible results.[101]

Carrageenan Phantoms

Carrageenan is a gelling agent obtained from refined natural polymeric substances extracted from red algae. This material is composed of saccharides with molecular weights of 100 to 500 kDa consisted mainly of galactose and 3,6-anhydrogalactose.[99] During the gelation process, the molecular chains of carrageenan form a double helix and aggregate via sulfuric acid groups.

Table 12. The Ingredients and Properties of Gellan Gum Phantoms Proposed in the Literature.

	Miyakawa et al. (1995)[81]	King et al. (2007)[101]
Gellan gum	0.30 (% w/w)	1.50
NaCl	0.50 (% w/w)	—
NISAA	1 (% w/w)	—
Calcium chloride dihydrate	—	0.40
Potassium sorbate	—	0.10
1-Propanol	—	11.25 (% v/v)
Aluminum oxide powder	—	0.90 (< 1μm) 0.90 (1-2 μm) 0.90 (10-44 μm)
Water	The rest	The rest
f (MHz)	—	1-8
T (°C)	—	22
ρ ($Kg{\cdot}m^{-3}$)	—	1060 ± 30[a]
C ($kJ{\cdot}Kg^{-1}{\cdot}C^{-1}$)	—	3.66 ± 0.0[a]
κ ($W{\cdot}m^{-1}{\cdot}C^{-1}$)	—	0.58 0.57 ± 0.02[a]
D ($mm^2{\cdot}s^{-1}$)	—	0.15
α ($dB{\cdot}cm^{-1}$)	—	$0.53f^{1.04}$ 0.58[a]
c ($m{\cdot}s^{-1}$)	—	1561 1560[a]
B/A	—	8[a]
Backscatter coefficient ($cm^{-1}{\cdot}Sr^{-1}$)	—	1.79×10^{-5} (at 3 MHz)

The amounts of ingredients are presented in % w/v, unless otherwise specifically stated. NISAA = non-ionic surface active agent.
[a]Data were measured by Hariharan et al. (2007).[17]

Phantom recipes. The first carrageenan phantom was developed by Yoshimura et al. (2003) for MRI studies.[102] This phantom was mainly composed of carrageenan as a gelling agent, $GdCl_3$ as T_1 modifier, agarose as T_2 modifier, and NaN_3 as preservative. The T_1 and T_2 values of the phantom could be adjusted in the ranges of 202 to 1904 ms and 38 to 423 ms by varying the concentrations of $GdCl_3$ (from 0-140 $mmol{\cdot}kg^{-1}$) and agarose (0%-1.6%), respectively. The thermal and mechanical properties of carrageenan gel (e.g. melting temperature, gel strength, and elastic modulus) could be tuned by adding salts such as NaCl, KCl, and $CaCl_2$.[103] NaCl could also be used to adjust the electrical conductivity of this gel. The dielectric properties (ε'_r and σ) of carrageenan gel are increased linearly with NaCl concentrations, while these values are minimally affected by agarose and $GdCl_3$. Moreover, both dielectric constant and electrical conductivity of this phantom are positively correlated with applied frequency (5-130 MHz).[104]

In further research, a hybrid phantom gel using carrageenan and gellan gum was developed to overcome the shortcoming of each gel and integrate their favorable properties (e.g., transparency of gellan gum and mechanical strength of carrageenan).[99] This phantom, which is ma inly composed of carrageenan (0.8% w/w), gellan gum (0.2% w/w), potassium chloride (0.42% w/w, σ modifier), butanol (4% v/w, T_{CP} controller), sodium azide (0.03% w/w, preservative), and water, could exhibit reversible heat-sensitivity when a sufficient ratio of a NISAA (1.5% v/w) was incorporated in its recipe.[99]

Advantages and limitations. Carrageenan is more elastic and more resistant to cracking compared to agar, and thus it can be formed into various shapes without the need for reinforcing materials.[103] However, carrageenan phantoms undergo liquefaction at low temperatures (e.g., around 60°C), causing difficulties in visualization of the thermal coagulation. Therefore, these phantoms are only suitable for hyperthermia studies where temperatures below 50°C are applied. Significant alteration of electrical properties and the clouding point by water loss is another drawback of these materials. The phantoms could be maintained for several weeks when thoroughly sealed to prevent the water loss from their structures.[99]

Alginate Phantoms

Alginate is a polysaccharide obtained from brown seaweed. This material is a copolymer of D-mannuronic acid (M) and L-guluronic acid (G) that forms a gel in the presence of certain divalent cations such as calcium, strontium, or barium. The alginate gelation occurs as blocks of guluronic acid bind to other G blocks via divalent cations. The mechanical properties of alginates strongly depend on the G content, the length of the G blocks, and molecular weight.[105]

Phantom recipes. One of the first alginate thermal phantoms was developed using a sodium alginate with mean G/M ratio of 70% and mean molecular weight of 180 kDa. This gel was able to retain its stiffness and physical structure during LIT experiments. For preparation of this phantom, the aqueous solution of sodium alginate (3% w/v) was cross-linked with calcium chloride ($CaCl_2$, 80 mM) to obtain the final gel.[106] This phantom showed a thermal conductivity value (0.5737 $W{\cdot}m^{-1}{\cdot}K^{-1}$) close to that of human tissue (0.50-0.58 $W{\cdot}m^{-1}{\cdot}K^{-1}$).[9] The cell viability test with a sodium alginate phantom containing multi-walled carbon nanotubes (CNTs; 0.02% w/v) showed a laser penetration depth (δ) of 1.5 mm.[106] Introduction of CNTs into the tissue phantoms also increased the optical absorption, causing an improved optothermal heating.[107] Another sodium alginate phantom containing 3 $g{\cdot}mL^{-1}$ sodium alginate, 1 $mg{\cdot}mL^{-1}$ polystyrene microbeads, and 40 $mg{\cdot}mL^{-1}$ talc-France powder has also been proposed.[107] The optical properties of this phantom (μ_a= 1.04-0.06 mm^{-1}, and μ_s' = 0.05-0.07 mm^{-1}) at wavelength of 900 nm were correspondent with those of breast tumor tissue.

Advantages and limitations. Alginate phantoms are attractive candidates for laser ablation studies because of their favorable optical properties. These phantoms also exhibit suitable mechanical and thermal stability during the high-temperature studies. However, the gelation kinetic of alginates is difficult to control, which may result in heterogeneous structures. More uniform structures can be achieved through the use of $CaCO_3$-D-glucono-δ-lactone (GDL) and $CaCO_3$-GDL-$CaSO_4$ instead of $CaCl_2$. These substances significantly decrease the gelation rate because of a lower solubility of $CaCO_3$ compared with $CaCl_2$, allowing the alginate suspension to be molded prior to gelation.[108] However, in spite of this finding, the $CaCO_3$-GDL-$CaSO_4$ cross-linking agents have not been used so far for fabrication of thermal phantoms. The gelation rate of alginate hydrogels can also be controlled by adjusting the $CaCO_3$:$CaSO_4$ molar ratio, calcium content, polymer concentration, and temperature.[108]

Table 13 summarizes the various advantages and limitations of the thermal phantoms described in this study. This study intended to provide an overview of the gelling agents that have been specifically used in fabrication of thermal phantoms for hyperthermia and thermal ablation studies. Although a number of other gelling agents such as polyvinyl alcohol[55,109] may also show potential as thermal phantoms, they have, however, been rarely used in high-temperature regimes. Furthermore, their critical properties have not been thoroughly characterized. Assessment of

Table 13. A Brief Comparison of Various Gelling Agents Described in This Study.

	Advantages	Limitations	Suggested Use
TX-150	Simulation of high-water-content tissues at a wide frequency range Controllable physical properties Facile construction	Inability to simulate low-water-content tissues Variable gelation parameters Limited shelf life Unavailability of acoustic and optical values	1. RF 2. MW
Agar	Thermal stability Mechanical strength Applicable in a wide frequency range Adjustable physical properties Capability of producing heterogeneous structures Useful in construction of perfused phantoms	High opacity Low permittivity Low cavitation threshold	1. RF 2. MW 3. HIFU 4. LIT
PAA	Optical transparency Thermal stability Mechanical strength High formability Applicable for construction of heat-sensitive phantoms Adjustable physical properties Heat-sensitive perfused phantoms Appropriate cavitation threshold range	Toxic ingredients High cost of preparation Complicated construction process Limited shelf life	1. HIFU 2. RF 3. MW 4. LIT
HEC	Desirable dielectric properties Facile preparation High durability	Unavailability of acoustic and optical values	1. MW 2. RF
Gelatin	Ease of construction Low-cost ingredients Long-term stability Applicable in fabrication of heterogeneous structures	Low melting point Insufficient mechanical strength. High opacity level	1. LIT 2. MW 3. RF
GGM	Sufficient transparency Thermal stability Low ratio of gelling agent needed for gelation Formation of highly homogeneous structure	Difficulties in reproducibility of acoustic and thermal values Fragility Unavailable optical and acoustic properties.	1. RF 2. MW 3. HIFU
CAG	Desirable mechanical properties	Opacity Low melting point Limited shelf life	1. RF 2. MW
ALG	Mechanical stiffness High melting point Desirable optical properties	Unavailability of thermal, electrical, and acoustic properties	LIT

RF = radiofrequency; MW = microwave; HIFU = High Intensity Focused Ultrasound; LIT = Laser-induced thermal ablation; PAA = polyacrylamide; HEC = hydroxyethyl cellulose; GGM = gellan gum; CAG = carrageenan; ALG = alginate phantom.

various thermal, electrical, acoustic, and optical properties of these materials is an ongoing area of research, which will be critical for their potential application in high-temperature studies.

It is also important to note that the thermal, electrical, acoustic, and optical values of the phantoms presented in this study may significantly vary if recalculated in further studies because of differences in the applied laboratory conditions.

Discussion and Conclusion

Phantoms that closely mimic the various properties of human tissues play an important role in pre-clinical evaluation of diagnostic and therapeutic modalities. In spite of the commercial availability of numerous tissue-mimicking phantoms, customized tissue substitutes continue to have a role, especially in specific applications such as thermal therapy. In this therapeutic approach, in addition to general factors such as reproducibility, low cost of production, ease of fabrication, and non-toxicity, an ideal thermal phantom must exhibit tissue equivalency in thermal, electrical, acoustic, and optical properties as well as thermal stability at high temperatures. The capability of a thermal phantom to provide a three-dimensional visualization of the heat damage is another significant factor that allows a more facile and accurate evaluation of thermal modalities. However, because of the difficulties in representation of all the target tissue characteristics, the phantom recipes are mostly tuned to only simulate properties that are critical for intended experimental conditions (e.g., thermal and acoustic properties for HIFU experiments). Therefore, understanding of the thermal, electrical, acoustic, and optical properties of various thermal phantoms is crucial in selection of an appropriate recipe for a specific experimental setup. This article reviewed the key aspects of the phantoms that have been previously proposed for thermal therapy applications, with particular focus on the phantoms in gel state.

Polyacrylamide, agar, and gelatin are the most widely used materials for the preparation of thermal phantoms. The attractive properties of polyacrylamide phantoms are optical transparency, mechanical stability, formability into complex shapes, and ability to simulate the physical properties of biological tissues in wide frequency and temperature ranges. The main drawbacks of acrylamide are toxicity, limited shelf life, and complicated fabrication procedure. On the contrary, agar phantoms are simple to prepare, stable at high temperatures, and non-toxic. However, these phantoms are non-transparent to optical beams that prevent the visualization of coagulation region inside the phantoms. Gelatin phantoms also exhibit desirable features including bio-compatibility, bio-degradability, non-immunogenicity, long-term stability, ease of production, and commercial availability at relatively low costs. Nevertheless, these gels possess low melting temperatures, making them impractical for thermal ablation studies. In addition, gelatin thermal phantoms could not present the same mechanical strength as acrylamide or agar phantoms. The other tissue-mimicking materials described in this study included TX-150, Hydroxyethyl Cellulose, Gellan gum, Carrageenan, and Alginates. However, in spite of showing desirable physical properties, these materials have not been widely used in hyperthermia and thermal ablation studies, and their critical properties have not been sufficiently established. Further studies are necessary for well characterization of these materials in various aspects that are crucial in thermal therapy experiments. The academic and industry research groups are continuously developing new thermal phantoms to more accurately mimic the properties of various biological tissues, increasing the flexibility as well as reducing the cost of experiments.

Declaration of Conflicting Interests

The author(s) declared no potential conflicts of interest with respect to the research, authorship, and/or publication of this article.

Funding

The author(s) disclosed receipt of the following financial support for the research, authorship, and/or publication of this article: This work was supported by the Ministry of Science, Technology, and Innovation (MOSTI) Malaysia (Science Fund 06-01-03-SF0587).

References

1. Madsen EL, Dong F, Frank GR, Garras BS, Wear KA, Wilson T, et al. Interlaboratory comparison of ultrasonic backscatter, attenuation, and speed measurements. J Ultrasound Med. 1999;18:615-31.
2. Wear KA, Stiles TA, Frank GR, Madsen GL, Cheng F, Feleppa EJ, et al. Interlaboratory comparison of ultrasonic backscatter coefficient measurements from 2 to 9 MHz. J Ultrasound Med. 2005;24: 1235-50.
3. Anderson JJ, Herd MT, King MR, Haak A, Hafez ZT, Song J, et al. Interlaboratory comparison of backscatter coefficient estimates for tissue-mimicking phantoms. Ultrason Imaging. 2010;32:48-64.
4. Craciunescu OI, Howle LE, Clegg ST. Experimental evaluation of the thermal properties of two tissue equivalent phantom materials. Int J Hyperthermia. 1999;15:509-18.
5. Prakash P, Converse MC, Mahvi DM, Webster JG. Measurement of the specific heat capacity of liver phantom. Physiol Meas. 2006;27:N41-6.
6. Divkovic GW, Liebler M, Braun K, Dreyer T, Huber PE, Jenne JW. Thermal properties and changes of acoustic parameters in an egg white phantom during heating and coagulation by high intensity focused ultrasound. Ultrasound Med Biol. 2007;33:981-6.
7. Leonard JB, Foster KR, Athley TW. Thermal properties of tissue equivalent phantom materials. IEEE Trans Biomed Eng. 1984;BME-31:533-6.
8. Davidson SR, Sherar MD. Measurement of the thermal conductivity of polyacrylamide tissue-equivalent material. Int J Hyperthermia. 2003;19:551-62.
9. Sarkar S, Zimmermann K, Leng W, Viveksland P, Zhang J, Dorn H, et al. Measurement of the thermal conductivity of carbon nanotube–tissue phantom composites with the hot wire probe method. Ann Biomed Eng. 2011;39:1745-58.
10. Bini MG, Ignesti A, Millanta L, Olmi R, Rubino N, Vanni R. The polyacrylamide as a phantom material for electromagnetic hyperthermia studies. IEEE Trans Biomed Eng. 1984;31:317-22.
11. Okawai H, Kobayashi K, Nitta S. An approach to acoustic properties of biological tissues using acoustic micrographs of attenuation constant and sound speed. J Ultrasound Med. 2001;20:891-907.
12. Lafon C, Khokhlova VA, Kaczkowski PJ, Bailey MR, Sapozhnikov OA, Crum LA. Use of a bovine eye lens for observation of HIFU-induced lesions in real-time. Ultrasound Med Biol. 2006;32:1731-41.
13. Ortega R, Téllez A, Leija L, Vera A. Measurement of ultrasonic properties of muscle and blood biological phantoms. Phys Procedia. 2010;3:627-34.
14. Johnson H, Graham M. High Speed Signal Propagation: Advanced Black Magic. New Jersey, NJ: Prentice Hall; 2003; pp. 29-120.
15. Labuda CP, Church CC. Augmentation of HIFU-induced heating with fibers embedded in a phantom. Ultrasound Med Biol. 2011;37:442-9.
16. Canney MS, Khokhlova VA, Bessonova OV, Bailey MR, Crum LA. Shock-induced heating and millisecond boiling in gels and tissue due to high intensity focused ultrasound. Ultrasound Med Biol. 2010;36:250-67.
17. Hariharan P, Myers MR, Banerjee RK. HIFU procedures at moderate intensities—effect of large blood vessels. Phys Med Biol. 2007;52:3493-513.
18. Choi SY, Kim YS, Seo YJ, Yang J, Choi KS. Gas-filled phospholipid nanoparticles conjugated with gadolinium play a role as a potential theragnostics for MR-guided HIFU ablation. PLoS ONE. 2012;7:e34333.
19. Guy AW. Analyses of electromagnetic fields induced in biological tissues by thermographic studies on equivalent phantom models. IEEE Trans Microw Theory Tech. 1971;16:205-14.
20. Vitkin IA, Moriarty JA, Peters RD, Kolios MC, Gladman AS, Chen JC, et al. Magnetic resonance imaging of temperature changes during interstitial microwave heating: a phantom study. Med Phys. 1997;24:269-77.

21. Faraone A, Balzano Q, Simunic D. Experimental dosimetry in a sphere of simulated brain tissue near a half-wave dipole antenna. In: IEEE Symposium on Electromagnetic Compatability, (ed. IEEE-EMC Society), Denver, CO, 24-28 August 1998, pp. 906-11.
22. Kanda MY, Ballen M, Salins S, Chung-Kwang C, Balzano Q. Formulation and characterization of tissue equivalent liquids used for RF densitometry and dosimetry measurements. IEEE Trans Microw Theory Tech. 2004;52:2046-56.
23. Li Z, Vogel M, Maccarini PF, Stakhursky V, Soher BJ, Craciunescu OI, et al. Improved hyperthermia treatment control using SAR/temperature simulation and PRFS magnetic resonance thermal imaging. Int J Hyperthermia. 2011;27:86-99.
24. Bu-Lin Z, Bing H, Sheng-Li K, Huang Y, Rong W, Jia L. A polyacrylamide gel phantom for radiofrequency ablation. Int J Hyperthermia. 2008;24:568-76.
25. Schepps JL and Foster KR, The UHF and microwave dielectric properties of normal and tumour tissues. variation in dielectric properties with tissue water content. Phys Med Biol. 1980;25:1149-59.
26. Robinson MP, Richardson MJ, Green JL, Preece AW. New materials for dielectric simulation of tissues. Phys Med Biol. 1991;36:1565-71.
27. Gabriel S, Lau RW, Gabriel C. The dielectric properties of biological tissues: III. Parametric models for the dielectric spectrum of tissues. Phys Med Biol. 1996;41:2271-93.
28. Lazebnik M, Madsen EL, Frank GR, Hagness SC. Tissue-mimicking phantom materials for narrowband and ultrawideband microwave applications. Phys Med Biol. 2005;50:4245-58.
29. Ozen S, Koylu H. Phantom model of human brain tissue for cellular phone frequencies in electromagnetic field radiation absorption studies. GU J Sci. 2005;18:193-200.
30. Gabriel C, Gabriel S, Corthout E. The dielectric properties of biological tissues: I. Literature survey. Phys Med Biol. 1996;41:2231-49.
31. Pogue BW, Patterson MS. Review of tissue simulating phantoms for optical spectroscopy, imaging and dosimetry. J Biomed Opt. 2006;11:041102.
32. Cheong WF, Prahl SA, Welch AJ. A review of the optical properties of biological tissues. IEEE J Quant Electron. 1990;26:2166-85.
33. Vogel A, Venugopalan V. Mechanisms of pulsed laser ablation of biological tissues. Chem Rev. 2003;103:577-644.
34. Elliott AM, Stafford RJ, Schwartz J, Wang J, Shetty AM, Bourgoyne C, et al. Laser-induced thermal response and characterization of nanoparticles for cancer treatment using magnetic resonance thermal imaging. Med Phys. 2007;34:3102-8.
35. Iizuka MN, Vitkin IA, Kolios MC, Sherar MD. The effects of dynamic optical properties during interstitial laser photocoagulation. Phys Med Biol. 2000;45:1335-57.
36. Matvienko A, Mandelis A, Abrams S. Robust multiparameter method of evaluating the optical and thermal properties of a layered tissue structure using photothermal radiometry. Appl Opt. 2009;48:3192-203.
37. Madsen SJ, Patterson MS, Wilson BC. The use of India ink as an optical absorber in tissue-simulating phantoms. Phys Med Biol. 1992;37:985-93.
38. Dimofte A, Finlay JC, Zhu TC. A method for determination of the absorption and scattering properties interstitially in turbid media. Phys Med Biol. 2005;50:2291-311.
39. van Dongen KW, Verweij MD. A feasibility study for non-invasive thermometry using non-linear ultrasound. Int J Hyperthermia. 2011;27:612-24.
40. Culjat MO, Goldenberg D, Tewari P, Singh RS. A review of tissue substitutes for ultrasound imaging. Ultrasound Med Biol. 2010;36:861-73.
41. Brace CL. Radiofrequency and microwave ablation of the liver, lung, kidney, and bone: what are the differences? Curr Probl Diagn Radiol. 2009;38:135-43.
42. Edwards DW. U.S. Patent 3653996. Houston, TX: Atlas Chemicals Industries; 1972.
43. Cheung AY, Koopman DW. Experimental development of simulated biomaterials for dosimetry studies of hazardous microwave radiation (Short Papers). IEEE Trans Microw Theory Tech. 1976;24:669-73.
44. Chou CK, Chen GW, Guy AW, Luk KH. Formulas for preparing phantom muscle tissue at various radiofrequencies. Bioelectromagnetics. 1984;5:435-41.

45. Johnson D, Zderic V. Design and construction of a flow phantom for HIFU research. In: IEEE Ultrasonics Symposium (ed. MP Yuhas), New York, NY, 28-31 October 2007, pp. 1294-6.
46. Huang J, Holt RG, Cleveland RO, Roy RA. Experimental validation of a tractable numerical model for focused ultrasound heating in flow-through tissue phantoms. J Acoust Soc Am. 2004;116:2451.
47. Ishida T, Kato H. Muscle equivalent agar phantom for 13.56MHz RF-induced hyperthermia. Shimane J Med Sci. 1980;4:134-40.
48. Ito K, Furuya K, Okano Y, Hamada L. Development and characteristics of a biological tissue-equivalent phantom for microwaves. Electron Comm Jpn (Part I). 2001;84:67-77.
49. Takimoto T, Onishi T, Saito K, Takahashi M, Uebayashi S, Ito K. Evaluation on biological tissue equivalent agar-based solid phantoms up to 10 GHz—aiming at measurement of characteristics of antenna for UWB communications. In: Proceedings of ISAP (ed. IEICE), Seoul, South Korea, 3-5 August 2005, pp. 483-6.
50. Kato H, Hiraoka M, Ishida T. An agar phantom for hyperthermia. Med Phys. 1986;13:396-8.
51. Kato H, Ishida T. Development of an agar phantom adaptable for simulation of various tissues in the range 5-40 MHz. Phys Med Biol. 1987;32:221-6.
52. Zhou T, Meaney PM, Fanning MW, Geimer SD, Paulsen KD. Integrated microwave thermal imaging system with mechanically steerable HIFU therapy device. In: Proceedings of SPIE, Energy-Based Treatment of Tissue and Assessment V (ed. TP Ryan), San Jose, CA, 25-26 January 2009, p. 71810J.
53. Kao TJ, Saulnier GJ, Isaacson D, Szabo TL, Newell JC. A versatile high-permittivity phantom for EIT. IEEE Trans Biomed Eng. 2008;55:2601-7.
54. Burlew MM, Madsen EL, Zagzebski JA, Banjavic RA, Sum SW. A new ultrasound tissue-equivalent material. Radiol. 1980;134:517-20.
55. Holt RG, Roy RA. Measurements of bubble-enhanced heating from focused, MHz-frequency ultrasound in a tissue-mimicking material. Ultrasound Med Biol. 2001;27:1399-412.
56. Farny CH, Holt RG, Roy RA. The correlation between bubble-enhanced HIFU heating and cavitation power. IEEE Trans Biomed Eng. 2010;57:175-84.
57. Rickey DW, Picot PA, Christopher DA, Fenster A. A wall-less vessel phantom for Doppler ultrasound studies. Ultrasound Med Biol. 1995;21:1163-76.
58. Madsen EL, Frank GR, Dong F. Liquid or solid ultrasonically tissue-mimicking materials with very low scatter. Ultrasound Med Biol. 1998;24:535-42.
59. Lai CY, Kruse DE, Caskey CF, Stephens DN, Sutcliffe PL, Ferrara KW. Noninvasive thermometry assisted by a dual-function ultrasound transducer for mild hyperthermia. IEEE Trans Ultrason Ferroelectr Freq Control. 2010;57:2671-84.
60. Poepping TL, Nikolov HN, Rankin RN, Lee M, Holdsworth DW. An in vitro system for Doppler ultrasound flow studies in the stenosed carotid artery bifurcation. Ultrasound Med Biol. 2002;28:495-506.
61. Cubeddu R, Pifferi A, Taroni P, Torricelli A, Valentini G. A solid tissue phantom for photon migration studies. Phys Med Biol. 1997;42:1971-9.
62. Elliott AM, Shetty AM, Wang J, Hazle JD, Jason Stafford R. Use of gold nanoshells to constrain and enhance laser thermal therapy of metastatic liver tumours. Int J Hyperthermia. 2010;26:434-40.
63. Iizuka MN, Sherar MD, Vitkin IA. Optical phantom materials for near infrared laser photocoagulation studies. Lasers Surg Med. 1999;25:159-69.
64. Siddiqi AK, Cho SH. Agar-based heat-sensitive gel with linear thermal response over 65–80 °C. J Therm Anal Calorim. 2013;111:1805-9.
65. Solazzo SA, Liu Z, Lobo SM, Ahmed M, Hines-Peralta AU, Lenkinski RE, et al. Radiofrequency ablation: importance of background tissue electrical conductivity—an agar phantom and computer modeling study. Radiol. 2005;236:495-502.
66. Liu Z, Ahmed M, Weinstein Y, Yi M, Mahajan RL, Goldberg SN. Characterization of the RF ablation-induced "oven effect": the importance of background tissue thermal conductivity on tissue heating. Int J Hyperthermia. 2006;22:327-42.
67. Ortega-Palacios R, Leija L, Vera A, Cepeda MFJ. Measurement of breast - tumor phantom dielectric properties for microwave breast cancer treatment evaluation. In: 7th International Conference on Electrical Engineering Computing Science and Automatic Control (CCE) (eds. JAM Cadenas, CA Coello, AP Gorbatch), Chiapas, Mexico, 8-10 September, pp. 216-9.

68. Andreuccetti D, Bini M, Ignesti A, Olmi R, Rubino N, Vanni R. Use of polyacrylamide as a tissue-equivalent material in the microwave range. IEEE Trans Biomed Eng. 1988;35:275-7.
69. Surowiec A, Shrivastava PN, Astrahan M, Petrovich Z. Utilization of a multilayer polyacrylamide phantom for evaluation of hyperthermia applicators. Int J Hyperthermia. 1992;8:795-807.
70. McDonald M, Lochhead S, Chopra R, Bronskill MJ. Multi-modality tissue-mimicking phantom for thermal therapy. Phys Med Biol. 2004;49:2767-78.
71. Park SK, Guntur SR, Lee KI, Paeng D-G, Choi MJ. Reusable ultrasonic tissue mimicking hydrogels containing nonionic surface-active agents for visualizing thermal lesions. IEEE Trans Biomed Eng. 2010;57:194-202.
72. Bazrafshan B, Hubner F, Farshid P, Larson MC, Vogel V, Mäntele W, et al. A liver-mimicking MRI phantom for thermal ablation experiments. Med Phys. 2011;38:2674-84.
73. Bouchard LS, Bronskill MJ. Magnetic resonance imaging of thermal coagulation effects in a phantom for calibrating thermal therapy devices. Med Phys. 2000;27:1141-5.
74. Lafon C, Zderic V, Noble ML, Yuen JC, Kaczkowski PJ, Sapozhnikov OA, et al. Gel phantom for use in high-intensity focused ultrasound dosimetry. Ultrasound Med Biol. 2005;31:1383-9.
75. Arora M, Arvanitis C, Cox E, Coussios CC. Localization and enhancement of cavitation and heating during HIFU exposure using microparticles of high surface roughness. J Acoust Soc Am. 2008;123:2997.
76. Zhang P, Porter T. An in vitro study of a phase-shift nanoemulsion: a potential nucleation agent for bubble-enhanced HIFU tumor ablation. Ultrasound Med Biol. 2010;36:1856-66.
77. Khokhlova VA, Bailey MR, Reed JA, Cunitz BW, Kaczkowski PJ, Crum LA. Effects of nonlinear propagation, cavitation, and boiling in lesion formation by high intensity focused ultrasound in a gel phantom. J Acoust Soc Am. 2006;119:1834-48.
78. Choi MJ, Guntur SR, Lee KI, Paeng DG, Coleman A. A tissue mimicking polyacrylamide hydrogel phantom for visualizing thermal lesions generated by high intensity focused ultrasound. Ultrasound Med Biol. 2013;39:439-48.
79. Lafon C, Kaczkowski PJ, Vaezy S, Noble M, Sapozhnikov OA. Development and characterization of an innovative synthetic tissue-mimicking material for high intensity focused ultrasound (HIFU) exposures. In: IEEE Ultrasonics Symposium (eds. DE Yuhas, SC Schneider), Atlanta, GA, 7-10 October 2001, pp. 1295-8.
80. Takegami K, Kaneko Y, Watanabe T, Maruyama T, Matsumoto Y, Nagawa H. Polyacrylamide gel containing egg white as new model for irradiation experiments using focused ultrasound. Ultrasound Med Biol. 2004;30:1419-22.
81. Miyakawa M, Takahashi N, Hoshina S. A method for observing the three-dimensional patterns of electromagnetic power absorbed by the human body-the gel phantom of the human body used to study the electromagnetic environmental problem. Electron Comm Jpn (Part I). 1995;78:99-112.
82. Miyakawa M, Hoshina S, Kanai Y. Visualization and 3-D measurement of local SAR using a gel phantom. In: IEEE Symposium on Electromagnetic Compatibility, (ed. IEEE-EMC Society), Denver, CO, 24-28 August 1998, pp. 751-6.
83. Dabbagh A, Abdullah BJJ, Abu Kasim NH, Ramasindarum C. Reusable heat-sensitive phantom for precise estimation of thermal profile in hyperthermia application. Int J Hyperthermia. 2014;30:66-74.
84. Jiang C, Wu MC, Wu YS. Inducing occlusion effect in Y-shaped vessels using high-intensity focused ultrasound: finite element analysis and phantom validation. Comput Methods Biomech Biomed Engin. 2012;15:323-32.
85. Kamel S, Ali N, Jahangir K, Shah SM, El-Gendy AA. Pharmaceutical significance of cellulose: a review. Express Polym Lett. 2008;2:758-78.
86. Hartsgrove G, Kraszewski A, Surowiec A. Simulated biological materials for electromagnetic radiation absorption studies. Bioelectromagnetics. 1987;8:29-36.
87. Stauffer PR, Rossetto F, Prakash M, Neuman DG, Lee T. Phantom and animal tissues for modelling the electrical properties of human liver. Int J Hyperthermia. 2003;19:89-101.
88. Yamamoto M, Ikada Y, Tabata Y. Controlled release of growth factors based on biodegradation of gelatin hydrogel. J Biomater Sci Polym Ed. 2001;12:77-88.
89. Bigi A, Cojazzi G, Panzavolta S, Roveri N, Rubini K. Stabilization of gelatin films by crosslinking with genipin. Biomaterials. 2002;23:4827-32.

90. Zhang YZ, Venugopal J, Huang ZM, Lim CT, Ramakrishna S. Crosslinking of the electrospun gelatin nanofibers. Polymer. 2006;47:2911-7.
91. Marchal C, Nadi M, Tosser AJ, Roussey C, Gaulard ML. Dielectric properties of gelatine phantoms used for simulations of biological tissues between 10 and 50 MHz. Int J Hyperthermia. 1989;5:725-32.
92. Nadi M, Marchal C, Rouane A, Hedjiedj A, Kourtiche D, Prieur G. Effect of temperature variations on the dielectric properties of a radiofrequency, gelatin water phantom. In: 14th International IEEE Engineering in Medicine and Biology Society Conference (eds. JP Morucci, R. Plonsey, JL Coatrieux, S Laxminarayan), Paris, France, 29 October 1992, pp. 268-9.
93. Yuan Y, Wyatt C, Maccarini P, Stauffer P, Craciunescu O, Macfall J, et al. A heterogeneous human tissue mimicking phantom for RF heating and MRI thermal monitoring verification. Phys Med Biol. 2012;57:2021-37.
94. Madsen EL, Frank GR, Krouskop TA, Varghese T, Kallel F, Ophir J. Tissue-mimicking oil-in-gelatin dispersions for use in heterogeneous elastography phantoms. Ultrason Imaging. 2003;25:17-38.
95. Lindner U, Lawrentschuk N, Weersink RA, Raz O, Hlasny E, Sussman MS, et al. Construction and evaluation of an anatomically correct multi-image modality compatible phantom for prostate cancer focal ablation. J Urol. 2010;184:352-7.
96. Baldock C, Burford RP, Billingham N, Wagner GS, Patval S, Badawi RD, et al. Experimental procedure for the manufacture and calibration of polyacrylamide gel (PAG) for magnetic resonance imaging (MRI) radiation dosimetry. Phys Med Biol. 1998;43:695-702.
97. Sunaga T, Ikehira H, Furukawa S, Tamura M, Yoshitome E, Obata T, et al. Development of a dielectric equivalent gel for better impedance matching for human skin. Bioelectromagnetics. 2003;24: 214-7.
98. Anderson PG, Rouze NC, Palmeri ML. Effect of graphite concentration on shear-wave speed in gelatin-based tissue-mimicking phantoms. Ultrason Imaging. 2011;33:134-42.
99. Kuroda M, Kato H, Hanamoto K, Shimamura K, Uchida T, Wang Y, et al. Development of a new hybrid gel phantom using carrageenan and gellan gum for visualizing three-dimensional temperature distribution during hyperthermia and radiofrequency ablation. Int J Oncol. 2005;27:175-84.
100. Caggioni M, Spicer PT, Blair DL, Lindberg SE, Weitz DA. Rheology and microrheology of a microstructured fluid: the gellan gum case. J Rheol. 2007;51:851-65.
101. King RL, Herman BA, Maruvada S, Wear KA, Harris GR. Development of a HIFU phantom. In: AIP, 6th International Symposium on Therapeutic Ultrasound (eds. C-C Coussios, G ter Haar), Oxford, UK, 30 August- 2 September 2006, pp. 351-6.
102. Yoshimura K, Kato H, Kuroda M, Yoshida A, Hanamoto K, Tanaka A, et al. Development of a tissue-equivalent MRI phantom using carrageenan gel. Magn Reson Med. 2003;50:1011-7.
103. Yoshida A, Kato H, Kuroda M, Hanamoto K, Yoshimura K, Shibya K, et al. Development of a phantom compatible for MRI and hyperthermia using carrageenan gel-relationship between T1 and T2 values and NaCl concentration. Int J Hyperthermia. 2004;20:803-14.
104. Kato H, Yoshimura K, Kuroda M, Yoshida A, Hanamoto K, Kawasaki S, et al. Development of a phantom compatible for MRI and hyperthermia using carrageenan gel—relationship between dielectric properties and NaCl concentration. Int J Hyperthermia. 2004;20:529-38.
105. Kellomaki M, Tormala P. Processing of resorbable poly-α-hydroxy acids for use as tissue-engineering scaffolds. Methods Mol Biol. 2004;238:1-10.
106. Fisher JW, Rylander MN. Effective cancer laser-therapy design through the integration of nanotechnology and computational treatment planning models. In: SPIE, Plasmonics in Biology and Medicine V Vol. 6869 (eds. T Vo-Dinh, JR Lakowiczoseph), San Jose, CA, 21-22 January 2008, p. 68690D.
107. Sarkar S, Gurjarpadhye AA, Rylander CG, Nichole Rylander M. Optical properties of breast tumor phantoms containing carbon nanotubes and nanohorns. J Biomed Opt. 2011;16:051304.
108. Kuo CK, Ma PX. Ionically crosslinked alginate hydrogels as scaffolds for tissue engineering: part 1. structure, gelation rate and mechanical properties. Biomaterials. 2001;22:511-21.
109. Zell K, Sperl J, Vogel M, Niessner R, Haisch C. Acoustical properties of selected tissue phantom materials for ultrasound imaging. Phys Med Biol. 2007;52:N475-84.